X. J. Fan[1]
Philips Research USA, 345 Scarborough Road, Briarcliff Manor, NY 10510
e-mail: xuejun.fan@ieee.org

J. Zhou
Department of Mechanical Engineering, Lamar University, Beaumont, TX 77710
e-mail: jenny.zhou@lamar.edu

G. Q. Zhang
Philips-CFT, P.O. Box 218, 5600 MD Eindhoven, The Netherlands
e-mail: g.q.zhang@philips.com

L. J. Ernst
Delft University of Technology, Mekelweg 2, 2628 CD Delft, The Netherlands
e-mail: l.j.ernst@wbmt.tudelft.nl

A Micromechanics-Based Vapor Pressure Model in Electronic Packages

A complete vapor pressure model based on a micromechanics approach is developed in this paper. The model can be extended to calculate the initial vapor pressure as traction loading subjected to the interfaces after the delamination. The impact of the vapor pressure induced expanison on the material's deformation is discussed.
[DOI: 10.1115/1.1939027]

1 Introduction

Polymer materials have wide applications in microelectronic packaging. Some polymer materials are used in bulk form, such as encapsulant (molding compound) and carrier or printed circuit boards (FR4 and BT). Some polymer materials are used as adhesives, such as die-attach, underfill, or other structural and thermal adhesives. Polymers are also used in thin or thick film as an isolation layer, such as a solder mask on a printed circuit board or passivation layer in the wafer level.

Despite the diversities of the chemistry and compositions, the polymer materials applied in microelectronics can be either thermoset or thermoplastic materials [1]. Both types of materials have a glass transition temperature around which the material properties, such as the CTE and Young's modulus, are very sensitive to temperature.

Another common feature of polymer materials is the high porosity, which makes the material susceptible to moisture absorption. In order to understand better the capacity of the moisture absorption by a typical polymer material, let us introduce some important parameters, which will be used frequently in subsequent sections, as follows:

- moisture concentration C, a measure of moisture distribution in material representing the mass of moisture per unit volume of the porous material
- saturated moisture concentration C_{sat}, the moisture concentration C in the fully saturated state
- moisture density ρ, the mass of moisture (and/or vapor) per unit volume of free spaces in material (defined by Eq. (1))
- ambient moisture density ρ_{ext}, a measure of moisture density in ambient
- saturated moisture density ρ_g, the maximum moisture density in air

Let us estimate how much moisture a polymer material could absorb. For a typical molding compound in 85°C/85RH ambient moisture condition, a typical value for the saturated moisture concentration is [2]

$$C_{\text{sat}} = 1.25 \times 10^{-2}\ \text{g/cm}^3$$

The saturated water vapor density at 85°C is

$$\rho_g = 3.576 \times 10^{-4}\ \text{g/cm}^3$$

such that at 85RH the ambient moisture density is

$$\rho_{\text{ext}} = 0.85 \times \rho_g = 3.04 \times 10^{-4}\ \text{g/cm}^3$$

It is straightforward to note $C_{\text{sat}} = \sim 41\rho_{\text{ext}}$, which means the apparent moisture density in the material is much higher than the ambient moisture density. With this observation it is inferred that most of the moisture in the (porous) material must be condensed into the mixed *liquid/vapor two-phase* state. In fact, the diffusion process of moisture is the transport process of moisture from ambient to material inside, characterized by mutual moisture condensation. The moisture is stored in micropores or free volumes in the material.

In this paper, an overview of the moisture diffusion analysis in multiple-material system is presented first. Then evaporation of the moisture during the temperature rise is studied based on a microvoid approach. The initial vapor pressure as traction loading subjected to the delamination interfaces is also investigated. The impact of vapor pressure-induced expansion on the material's deformation is discussed.

2 Moisture-Diffusion Analysis

Transient moisture diffusion follows the Fick's law as follows:

$$\frac{\partial^2 C^2}{\partial x^2} + \frac{\partial^2 C^2}{\partial y^2} + \frac{\partial^2 C^2}{\partial z^2} = \frac{1}{\alpha_D}\frac{\partial C}{\partial t} \tag{1}$$

where C is the local concentration (g/cm^3), x, y, z are coordinates (cm), α_D is the moisture diffusivity (cm^2/s), and t is the time (s). It was noted that the moisture concentration along the bimaterial interface is not continuous [2]. However, the partial vapor pressure at the interface and the flux of the moisture are continuous across the interface, as follows:

$$C_1/S_1 = C_2/S_2 \tag{2}$$

[1]Corresponding author current address: ATD Q&R, CH5-263, Intel Corporation, 5000 W. Chandler Blvd, Chandler, AZ 85226

Contributed by the Electronic and Photonic Packaging Division for publication in the JOURNAL OF ELECTRONIC PACKAGING. Manuscript received June 22, 2004; Final manuscript received June 26, 2004. Review conducted by: Bahgat Sammakia. Presented at the 3rd Int. Conf. on Thermal and Thermo-mechanical Simulation in Microelectronics, Paris, France, April 15–17, 2002.

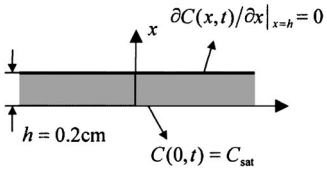

Fig. 1 One-dimensional transient moisture-diffusion problem

$$\alpha_{D1}\frac{\partial C_1}{\partial n}=\alpha_{D2}\frac{\partial C_2}{\partial n} \tag{3}$$

where 1 and 2 represent different materials, respectively, and S is the solubility. The solubility S is related to the saturated concentration C_{sat} by

$$S=C_{sat}/p_{ext} \tag{4}$$

where p_{ext} is the ambient vapor pressure under the given humid conditions.

In order to numerically solve Eq. (1) in a multiple-material system (e.g., by finite element method), the following variable with continuity at the interface can be defined [2]

$$\varphi=C/S \tag{5}$$

or equivalently, according to Eq. (4)

$$w=C/C_{sat} \tag{6}$$

In order to illustrate the nature of the moisture diffusion in plastic materials, we consider an example of a simple transient moisture diffusion problem in a slab, with the boundary conditions as shown in Fig. 1. The thickness of 2 mm is taken as a typical value. The material properties (e.g., a typical mold compound), together with the ambient humid conditions for three types of moisture preconditioning are listed in Table 1 [2]. The solution can be represented as [3]

$$C(x,t)=C_{sat}\left[1-\sum_{n=0}^{\infty}\frac{[2(-1)^n]e^{-\lambda_n^2\alpha_D t/h^2}}{\lambda_n}\cos(\lambda_n(h-x)/h)\right] \tag{7}$$

where

$$\lambda_n=\left(\frac{2n+1}{2}\right)\pi \tag{8}$$

Figure 2 plotted the results for the local moisture concentration at $x=h$ as the function of time. It takes hundreds of hours (or even longer) to the saturated moisture state. Assuming that the thermal diffusivity for this slab as 4.22×10^{-3} cm^2/s [4], Fig. 3 plotted the temperature rise at the side $x=h$ as function of time, when the side $x=0$ is suddenly subjected to a step-temperature rise ΔT. The results of Figs. 2 and 3 showed that the heat transfer is much faster than moisture diffusion. This implies that the package temperature can be approximately assumed as uniform at reflow temperature. The loss of moisture because of desorption during the process of reflow is negligible, since the solder reflow process is completed in a few minutes.

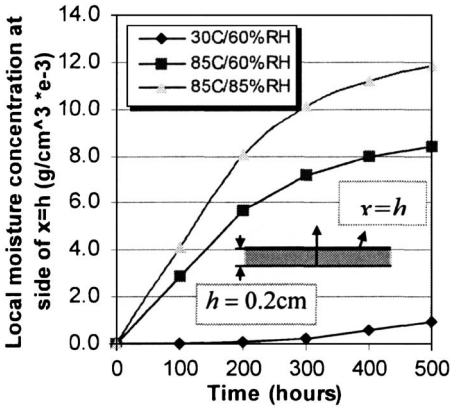

Fig. 2 Local moisture concentration at $x=h$ as function of time

3 Vapor Pressure Modeling: A Microvoid Approach

Previous studies assume that the moisture is always in a single vapor phase throughout the temperature rise [5], and hence the ideal gas law can be applied for the evolution of the internal vapor pressure inside voids. Since such a vapor pressure model is not linked to the moisture property of the material, it is difficult to estimate the initial or reference vapor presure at reference temperature (e.g., temperature T_0 at precoditioning). The problem becomes very complicated when the moisture in voids is at mixed liquid-vapor phase, which occurs in most of cases for polymer materials.

One of critical issues in developing a vapor pressure model is to find out the moisture density in *voids*, denoted as ρ,

$$\rho=\frac{dm}{dV_f} \tag{9}$$

where dm is the mass of moisture per unit volume of free spaces in material, dV_f. The moisture concentration C is defined as

$$C=\frac{dm}{dV} \tag{10}$$

where dV is the element volume of the porous material dV, which contains free spaces dV_f. It should be noted that, because of the inhomogeneous character of a porous material, the element should be established over a (finite) representative volume (RVE) [6].

Introducing the void volume fraction f [6] according to

Table 1 Three types of moisture preconditioning

Moisture preconditioning	Saturated vapor density ρ_g(g/cm^3)	Saturated vapor pressure p_g(MPa)	Ambient vapor density ρ_{ext}(g/cm^3)	Ambient vapor pressure p_{ext}(MPa)	Moisture diffusivity α_D(cm^2/s)	Saturated concentration C_{sat}(g/cm^3) $= p_{ext}S$
30°C/60%RH	3.04×10^{-5}	4.24×10^{-3}	$0.6\,\rho_g$	$0.6\,p_g$	3.13×10^{-9}	7.86×10^{-3}
85°C/60%RH	3.58×10^{-4}	5.87×10^{-2}	$0.6\,\rho_g$	$0.6\,p_g$	2.85×10^{-8}	8.84×10^{-3}
85°C/85%RH	3.58×10^{-4}	5.87×10^{-2}	$0.85\,\rho_g$	$0.85\,p_g$	2.85×10^{-8}	1.25×10^{-2}

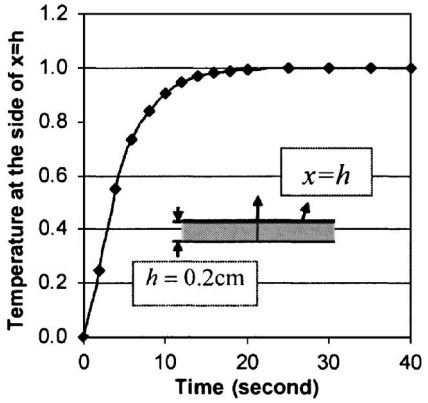

Fig. 3 Dimensionless temperature at $x=h$ as function of time

$$f = \frac{dV_f}{dV} \quad 0 < f \leq 1 \tag{11}$$

The following relation between ρ and C can be obtained

$$\rho = \frac{\mathrm{d}m}{\mathrm{d}V_f} = \frac{\mathrm{d}m}{\mathrm{d}V}\frac{\mathrm{d}V}{\mathrm{d}V_f} = C/f \tag{12}$$

As discussed before, the saturated moisture concentration $C_{\text{sat}} = 41\rho_{\text{ext}}$ at 85°C/85RH condition for a typical mold compound. Assume that the void volume fraction f is 0.05, Eq. (12) gives $\rho = 820\rho_{\text{ext}}$. This number clearly shows that how much moisture a typical polymer material could absorb. Such an amount of moisture must condense into the mixed liquid-vapor phase in material.

The following condition is used to determine the moisture state in voids at preconditioning of temperature T_0,

$$\begin{cases} \rho \leq \rho_g(T_0) & \text{for vapor phase at } T_0 \\ \rho > \rho_g(T_0) & \text{for mixed liquid/vapor phase at } T_0 \end{cases} \tag{13}$$

where ρ_g is the saturated vapor density, which can be obtained from the steam table as function of temperature.

When the moisture is at mixed liquid-vapor phase, it is necessary to know at which temperature the moisture can be *fully* vaporized. This temperature is called the *phase transition temperature*, denoted by T_1, which can be determined by

$$\rho(T_1) = \rho_g(T_1) \tag{14}$$

Now the vapor pressure in voids can be determined by the moisture state analyzed above. When the moisture is in the mixed liquid-vapor phase, the vapor pressure maintains the saturated vapor pressure p_g as function of temperature (from steam table), i.e.,

$$p(T) = p_g(T) \text{ for mixed liquid-vapor phase} \tag{15}$$

When the moisture is in single vapor phase, the ideal gas law can be followed to calculate the vapor pressure as follows:

$$p\mathrm{d}V_f = \mathrm{d}mRT \text{ or } p = \rho RT \tag{16}$$

Dividing both sides by dV, we obtain

$$pf = CRT \tag{17}$$

where R is the universal gas constant (=8.314 J/mol).

The two states (p,f,T,C) and (p_r,f_r,T_r,C_r) are then related by

$$\frac{p}{p_r} = \frac{Tf_rC}{T_rfC_r} \text{ for single vapor phase from } T_r \text{ to } T \tag{18}$$

Assume that the material is incompressible, the change of volume element due to the temperature change is related by [7]

$$\frac{dV}{dV_0} \approx 1 + 3\alpha\Delta T \tag{19}$$

where $\Delta T = T - T_0$ and α the coefficient of thermal expansion. Thus,

$$C = \frac{\mathrm{d}m}{\mathrm{d}V} = \frac{\mathrm{d}m}{\mathrm{d}V_0}\frac{\mathrm{d}V_0}{\mathrm{d}V} = C_0(1 - 3\alpha\Delta T) \tag{20}$$

from which, it is noted that although the moisture mass is assumed conserved during the temperature rise (the desorption effect is neglected), the moisture concentration may change due to the change of the bulk volume by thermal expansion.

Three distinct cases for the vapor pressure evolution have been identified [6–9], and are shown in Fig. 4. In the following, the detailed description and derivation for the vapor pressure evolution for each case are presented, and some corrections on the errors in previous publications are made.

In case 1, the moisture in void is in single vapor phase at T_0 after the moisture absoprtion. The condition for this case can be mathematically expressed as

$$\rho(T_0) \leq \rho_g(T_0) \tag{21}$$

or equivalently, according to Eq. (12)

$$C_0/f_0 \leq \rho_g(T_0) \tag{22}$$

The initial vapor pressure at T_0 can be determined from Eq. (16), by relating with a fully saturated state at temperature T_0, as follows:

$$p_0 = p(T_0) = \rho(T_0)RT_0$$

$$p_g(T_0) = \rho_g(T_0)RT_0 \tag{23}$$

thus,

$$p_0 = \frac{\rho(T_0)}{\rho_g(T_0)}p_g(T_0) = \frac{C_0p_g(T_0)}{f_0\rho_g(T_0)} \tag{24}$$

by which the vapor pressure at temperature T_0 can be calculated when the moisture concentration and the initial void volume fraction are known.

The vapor pressure at temperature T for case 1 can then be obtained from Eq. (18) with the reference state (p_r,f_r,T_r,C_r) to be substituted by (p_0,f_0,T_0,C_0), as follows:

$$p(T) = \frac{Tf_0C}{T_0fC_0}p_0 = \frac{C_0p_g(T_0)}{\rho_g(T_0)f}\frac{T}{T_0}[1 - 3\alpha(T - T_0)] \tag{25}$$

In case 2, the moisture in the voids is in the mixed liquid-vapor phase at *current* temperature T. Therefore, the moisture must also be in the mixed liquid-vapor phase at initial T_0. The condition for case 2 is thus as follows

$$\rho(T) \geq \rho_g(T) \tag{26}$$

or by Eq. (12)

$$\frac{C_0}{f}[1 - 3\alpha(T - T_0)] \geq \rho_g(T) \tag{27}$$

In this case the vapor pressure maintains the saturated vapor pressure during the course of the temperature rise. Thus the vapor pressure at temperature T follows Eq. (15) as follows:

$$p(T) = p_g(T) \tag{28}$$

Case 3 is an intermediate case between cases 1 and 2, where the moisture is in the mixed liquid-vapor phase at initial T_0, but in the single vapor phase at current T. The condition for this case can be written as

$$\rho(T_0) > \rho_g(T_0) \text{ and } \rho(T) < \rho_g(T) \tag{29}$$

or using Eq. (12)

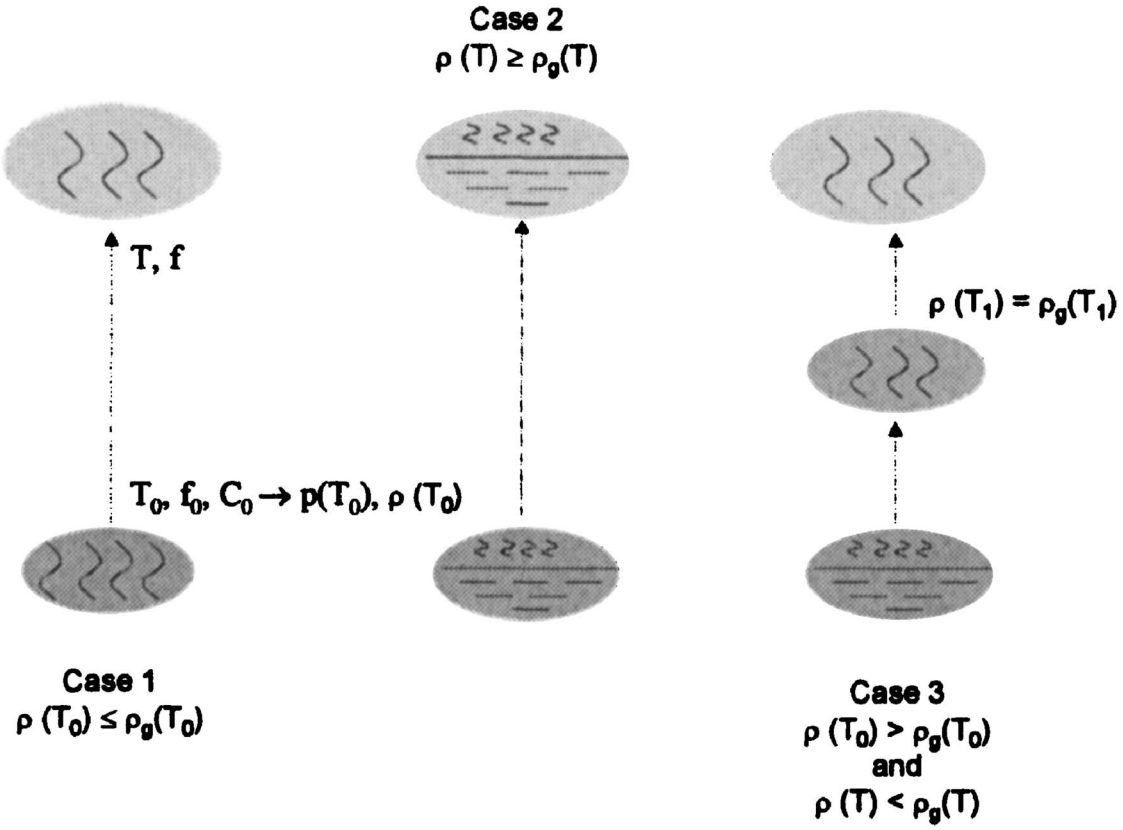

Fig. 4 Three distinct cases for the vapor pressure evolution from the preconditioning temperature T_0 to the current temperature T. In case 1, the moisture in the void is in the single vapor phase at T_0, thus the vapor pressure at T follows the ideal gas law. In case 2, the moisture in the void is in the mixed liquid-vapor phase at temperature T (must be in the mixed liquid-vapor phase at T_0, too), thus the vapor pressure maintains the saturated vapor pressure during the course of the temperature rise. Case 3 is an intermediate case between case 1 and case 2, where the moisture is in the mixed liquid-vapor phase at T_0, but in the single vapor phase at T. The phase transition temperature T_1 where the moisture is just fully vaporized should be determined first. Then the vapor pressure follows the ideal gas law from $T \geqslant T_1$. The complete equations are given in (33)–(35).

$$C_0/f_0 > \rho_g(T_0) \text{ and } \frac{C_0}{f}[1-3\alpha(T-T_0)] < \rho_g(T) \tag{30}$$

The phase transition temperature T_1, where the moisture is just fully vaporized, should be determined first according to Eq. (14), which can be rewritten as

$$\frac{C_0}{f(T_1)}[1-3\alpha(T_1-T_0)] = \rho_g(T_1) \tag{31}$$

Then from T_1 to temperature T the Eq. (18) can be used with the reference state (p_r, f_r, T_r, C_r) to be substituted by $(p(T_1), f(T_1), T_1, C(T_1))$, as follows:

$$p(T) = p(T_1)\frac{T}{T_1}\frac{f(T_1)C}{fC(T_1)} = p_g(T_1)\frac{T}{T_1}\frac{f(T_1)C}{fC(T_1)}$$

$$= p_g(T_1)\frac{T}{T_1}\frac{f(T_1)}{f}\frac{1-3\alpha(T-T_0)}{1-3\alpha(T_1-T_0)} \tag{32}$$

Now the equations for calculating the vapor pressure are complete, which can be summarized as follows:

Case 1: when $C_0/f_0 \leqslant \rho_g(T_0)$

$$p(T) = \frac{C_0 p_g(T_0)}{\rho_g(T_0) f}\frac{T}{T_0}[1-3\alpha(T-T_0)] \tag{33}$$

Case 2: when $(C_0/f)[1-3\alpha(T-T_0)] \geqslant \rho_g(T)$

$$p(T) = p_g(T) \tag{34}$$

Case 3: when $C_0/f_0 > \rho_g(T_0)$, and $(C_0/f)[1-3\alpha(T-T_0)] < \rho_g(T)$

$$p(T) = p_g(T_1)\frac{T}{T_1}\frac{f(T_1)}{f}\frac{1-3\alpha(T-T_0)}{1-3\alpha(T_1-T_0)} \tag{35}$$

where T_1 is determined by Eq. (31)

The above model includes an unknown f, the current void volume fraction. Obviously, the vapor pressure is dependent on the void-deformation behaviors and should be solved together with the governing equations of deformation.

Let us investigate the magnitude of vapor pressure for case 1, where the moisture is fully vaporized at preconditioning. Assuming that the preconditioning temperature T_0 is 85 °C, the *maximum* vapor pressure allowed in voids at T_0 is the saturated vapor pressure $p_g(T_0=85\,^\circ\text{C}) = 5.27\times10^{-2}$ MPa. The vapor pressure at reflow temperature $T=220\,^\circ$C is plotted as function of the current void volume fraction f in Fig. 4, by using Eq. (33) ($\alpha = 200$ ppm/ °C, $f_0=0.03$). The vapor pressure decreases with the current void volume fraction. The pressure may be lower than the initial vapor pressure of T_0 when the void becomes large. The maximum vapor pressure developed at 220 °C is 7.92×10^{-2} MPa, when the void does not grow ($f=f_0$). The results imply that the vapor pressure for *case 1* is substantially low such that it has almost negligible effect on the void growth.

Consider the case 2 where the moisture is not fully vaporized at reflow temperature T. In this case the vapor pressure is the satu-

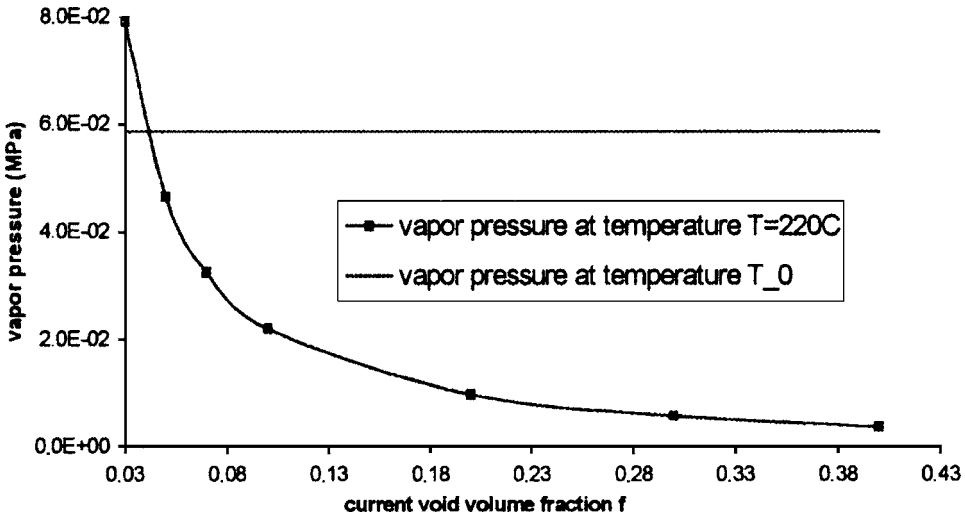

Fig. 5 Vapor pressure p at 220°C versus the current void volume fraction f by Eq. (35) for case 1, with $f_0=0.03$, $\alpha=200$ ppm/°C, $T_0=85$°C, and $p_0=p_{0\max}=p_g(85°C)=5.27\times10^{-2}$ MPa. It shows that the vapor pressure for case 1 is substantially low and has almost a negligible effect on the void growth.

rated vapor pressure, i.e., $p=p_g(T=220°C)=2.32$ MPa. The vapor pressure with such a magnitude has significant effect on the void behavior, which was discussed in Ref. [7].

Questions remain that how to measure the initial void volume fraction f_0. An approximate method in estimating the initial void volume fraction was proposed [6] by using the moisture absorption test. From Eq. (12), when moisture absorption is saturated, the initial void volume fraction is given by

$$f_0=\frac{C_{\text{sat}}}{\rho} \tag{36}$$

Given the fact that the moisture condenses mostly into the liquid form and the water liquid density is 1.0 g/cm^3, f_0 can be estimated from

$$f_0 \approx C_{\text{sat}}\big|_{100°C/100RH} \tag{37}$$

Equation (37) provides a simple way to predict the approximate magnitude of the voids fraction existing in polymer materials using the moisture property data given by Galloway et al. [2]. It shows that the initial void volume fraction is usually between 0.01 and 0.05.

Equation (20) can be simplified as $C\approx C_0$, since the thermal expansion is much smaller than 1. Equations (33)–(35) can then be simplified as follows:

Case 1: when $C_0/f_0\leqslant\rho_g(T_0)$

$$p(T)=\frac{C_0 p_g(T_0)}{\rho_g(T_0)f}\frac{T}{T_0} \tag{38}$$

Case 2: when $C_0/f\geqslant\rho_g(T)$

$$p(T)=p_g(T) \tag{39}$$

Case 3: when $C_0/f_0>\rho_g(T_0)$, and $C_0/f<\rho_g(T)$

$$p(T)=p_g(T_1)\frac{T}{T_1}\frac{f(T_1)}{f} \tag{40}$$

4 Vapor Pressure as External Loading in Delamiantated Area

The internal vapor pressure in voids at the interfaces instantaneously become an external pressure subjected to the delaminated interfaces when delamination is formed at reflow. By Eq. (11), the delamination is defined when $f=1$, which implies that the material element is totally voided. The initial vapor pressure subjected to the delaminated surfaces thus can be obtained from the above analysis with a special case $f=1$. This makes the problem simpler since the final state of the void growth is known already. By substituting $f=1$ into Eq. (38) and (40), we obtain

Case 1: when $C_0/f_0\leqslant\rho_g(T_0)$,

$$p(T)=\frac{C_0 p_g(T_0)}{\rho_g(T_0)}\frac{T}{T_0} \tag{41}$$

Case 2: when $C_0\geqslant\rho_g(T)$

$$p(T)=p_g(T) \tag{42}$$

Case 3: when $C_0/f_0>\rho_g(T_0)$, and $C_0<\rho_g(T)$

$$p(T)=p_g(T_1)f(T_1)\frac{T}{T_1} \tag{43}$$

where T_1 is determined by Eq. (31), and $T_0<T<T_1$.

The vapor pressure at the delaminated area will be immediately uniform when the delamination is complete, although the local moisture concentrations at interfaces are different with the location. Thus, the average local concentration can be defined as follows:

$$C^{\text{ave}}=\frac{\int_A CdA}{A} \tag{44}$$

where A is the delaminated area. In calculating the vapor pressure after delamination by above equations, the concentration C should be replaced by C^{ave}.

One of main differences between Eq. (41)–(43) and Eq. (38)–(40) is that the initial vapor pressure subjected to the delaminated surfaces can be computed directly, without knowing the deformation history of the voids, except for Eq. (43). For example, assuming that the void volume fraction is 0.03, if the local moisture concentration $C_0\leqslant f_0\rho_g(T_0)=0.03\times3.58\times10^{-4}=0.11\times10^{-4}$ g/cm^3 (under 85°C), then the vapor pressure can be calculated directly from Eq. (41). As indicated in Fig. 5, the vapor pressure in this case is substantially small such that it has negligible impact on the void growth. On the other hands, from Eq. (42), when the local concentration $C_0\geqslant\rho_g(T)=1.16\times10^{-2}$ g/cm^3 (under 220°C), the initial vapor pressure will remain the saturated vapor pressure 2.32 MPa. Equation (42) provides a very simple criterion for the vapor pressure estimation on

the delaminated surfaces. After the moisture-diffusion modeling is performed, the averaged moisture concentration can be calculated according to Eq. (44). When

$$C^{\text{ave}} \geqslant \rho_g(T) \tag{45}$$

the initial vapor pressure on the delaminated interface will remain the saturated vapor pressure at current temperature T according to Eq. (42). Otherwise, the vapor pressure will be dependent on the deformation history of the voids by Eq. (43).

5 Vapor Pressure-Induced Expansion

Our previous finite element modeling of whole field vapor pressure [9] according the to model developed above concludes that the vapor pressure saturated much faster than the moisture diffusion. This implies that the vapor pressure may be uniformly distributed in the plastic material regardless of moisture saturation. Young's modulus of plastic material drops a few orders at the reflow temperature, thus the vapor pressure-induced expansion may become as important as thermal expansion. For instance, assume Young's modulus of a typical underfill at 220°C is 500 MPa, and the Poisson ratio is 0.3. Therefore, the volume change caused by vapor pressure, $P_g(220\,^\circ\text{C})$ of 2.32 MPa, can be estimated as

$$\frac{\Delta V}{V} = \frac{3(1-2\nu)}{E} p = 5.568 \times 10^{-3} \tag{46}$$

which, is equivalent to the coefficient of thermal expansion (CTE) of $5.56\times10^{-3}/3/(220-175)=41$ ppm/°C under the 175–220°C temperature loading. The magnitude of this vapor pressure-induced strain is in the same order as thermal strain. It is obvious that the vapor pressure-induced expansion introduces additional mismatch. It must also be pointed out that such an expansion is directly related to the vapor pressure distribution, rather than the moisture distribution.

6 Conclusion

The moisture affects the package reliability at reflow from two aspects: generation of vapor pressure and degradation of interfacial adhesion. Although the vapor pressure remains at its saturated pressure when more moisture is absorbed, the adhesion strength may continuously deteriorate with additional moisture. When the interfacial adhesion is reduced to the level below the vapor pressure, the delamination will occur. This paper provides a complete model to describe the evolution of the vapor pressure in voids. Such a model can then be applied to a micromechanics analysis by considering the mechanisms of the interface strength degradation as function of temperature and moisture to give a complete analysis on the interface delamination induced by moisture, as discussed in Ref. [7].

The vapor pressure model presented in this paper also provides a consistent and easy criterion to estimate the initial vapor pressure after the delamination takes places. As long as the moisture concentration at the interface of interest exceeds the saturated water vapor density at the current temperature, the vapor pressure applied on the delaminated interface will remain the saturated vapor pressure. Other than this case, the vapor pressure evolution depends on the history of void deformation and a complete analysis from the void growth until the coalescence is necessary.

Appendix

Saturated water vapor density and vapor pressure at different temperatures

T(°C)	20	30	40	50	60	70	80
ρ_g(g/cm$^2\times10^{-3}$)	0.017	0.03	0.05	0.08	0.13	0.2	0.29
p_g(MPa)	0.002	0.004	0.007	0.01	0.02	0.03	0.05
T(°C)	90	100	110	120	130	140	150
ρ_g(g/cm$^2\times10^{-3}$)	0.42	0.6	0.83	1.12	1.5	1.97	2.55
p_g(MPa)	0.07	0.1	0.14	0.2	0.27	0.36	0.48
T(°C)	160	170	180	190	200	210	220
ρ_g(g/cm$^2\times10^{-3}$)	3.26	4.12	5.16	6.4	7.86	9.59	11.62
p_g(MPa)	0.62	0.79	1	1.26	1.55	1.91	2.32
T(°C)	230	240	250	260	270	280	290
ρ_g(g/cm$^2\times10^{-3}$)	14	16.76	19.99	23.73	28.1	33.19	39.16
p_g(MPa)	2.8	3.35	3.98	4.69	5.51	6.42	7.45

References

[1] Ernst, L. J., 2000, "Polymer Material Characterization and Modeling," in *Benefiting from Thermal and Mechanical Simulation in Microelectronics*, G. Q. Zhang et al., (eds.), Kluwer Academic, Boston, MA, pp. 37–58.

[2] Galloway, J. E., and Miles, B. M., 1997, "Moisture Absorption and Desorption Predictions for Plastic Ball Grid Array Packages," IEEE Trans. Compon., Packag. Manuf. Technol., Part A, **20**(3), pp. 274–279.

[3] Gebhart, B., 1993, *Heat Conduction and Mass Diffusion*, McGraw Hill, New York.

[4] Tay, A. A. O., and Lin, T., 1996, "Moisture Diffision and Heat Transfer in Plastic IC Packages," IEEE Trans. Compon., Packag. Manuf. Technol., Part A, **19**(2), pp. 186–193.

[5] Fan, X. J., and Zhang, S. Y., 1995, "Void Behavior Due to Internal Vapor Pressure Induced by Temperature Rise," J. Mater. Sci., **30**, pp. 3483–3489.

[6] Fan, X. J., and Lim, T. B., 1999, "Mechanism Analysis for Moisture-Induced Failure in IC Packages," *ASME Int. Mechanical Engineering Congress and Exposition, 11th Symp. on Mechanics of Surface Mount Technology*, Nashville, Tennessee, November, 14–19, IMECE/EPE-14.

[7] Fan, X. J., Zhang, G. Q., and Ernst, L. J., 2002, "A Micro-Mechanics Approach in Polymeric Material Failures in Microelectronic Packaging," *3rd Int. Conf. on Thermal and Thermo-Mechanical Simulation in Microelectronics*, pp. 154–164, April, 15–17.

[8] Fan, X. J., 2000, "Modeling of Vapor Pressure During Reflow for Electronic Packages," in *Benefiting from Thermal and Mechanical Simulation in Micro-Electronics*, G. Q. Zhang et al. (eds.), Kluwer Academic, Boston, MA, pp. 75–92.

[9] Tee, T. Y., and Fan, X. J., 1999, "Modeling of Whole Field Vapor Pressure During Reflow for Flip Chip BGA and Wire-Bond PBGA Packages," *1st Int. Workshop on Electronic Materials and Packaging*, Singapore, Sept. 29-Oct. 1, pp. 38–45.